BILINGUAL PUBLISHING CO.
Pioneer of Global Academics Since 1984

Journal of Geological Research
https://ojs.bilpublishing.com/index.php/jgr-a

ARTICLE

Geostatistical Modelling of Reservoir Quality Over "Bright" Field, Niger Delta

Abe, S.J* Olowokere, M. T Enikanselu, P. A

Department of Applied Geophysics, Federal University of Technology, Akure, Nigeria

ARTICLE INFO

Article history
Received: 14 January 2021
Accepted: 26 January 2021
Published Online: 31 January 2021

Keywords:
Probabilistic
Lp norm
Modelling
Gaussian
Stochastic

ABSTRACT

The quality of any hydrocarbon-bearing reservoir is vital for a successful exploitation work.. The reservoir quality is a function of its petrophysical parameters. Hence the need to model these properties geostatistically in order to determine the quality away from well locations.Composite logs for four wells and 3-D seismic data were used for the analysis. A reservoir named Sand X was mapped and correlated across wells 1 through 4. The four reservoir quality indicators - Effective porosity, permeability, volume of shale and net-to-gross- were estimated and modelled across the field. Sequential Gaussian simulation algorithm was employed to distribute these properties stochastically away from well locations and five realizations were generated. The volume of shale varied from 0.025 (Well 1, second realization) to 0.18(Well 2, first realization). The net-to-gross varied from 0.81 to 0.96 in wells 3 and 4 respectively, for the third realization, while the effective porosity varied from 0.125 to 0.295 for the fifth realization in Wells 3 and 4 respectively. The permeability is above 5000mD at all the existing well locations.These realizations were ranked using Lp norm statistical tool to pick the best for further evaluation. The reservoir quality deduced from the analyzed indicators was favourably high across the reservoir.The application of geostatistics has laterally enhanced the log data resolution away from established well locations.

1. Introduction

The quality of a reservoir is defined by its hydrocarbon storage capacity and deliverability. The hydrocarbon storage capacity is characterized by the effective porosity and the geometry of the reservoir, whereas the deliverability is a function of the permeability as well as the effective porosity or the volume percentage of interconnected pores in a rock. The remaining space in the rock is occupied by the framework or matrix of the rock and, if present, unconnected pore space.

Due to limited understanding of the details of many diagenetic processes, there is a lack of new techniques and tools to support reservoir quality predictions. Despite its notable economic importance, relatively few papers illustrate research in reservoir quality prediction. The main difficulty to execute this task is that the creation of models to reservoir quality prediction is highly dependent on quality and availability of calibration datasets [1,2]. Biased datasets will generate poor models. Furthermore, lack of observations combined to a high amount of features describing each observation can become more difficult, or even prohibitive, to fit a multivariate model to forecast

**Corresponding Author:*
Abe, S.J,
Department of Applied Geophysics, Federal University of Technology, Akure, Nigeria;
Email: jsabe@futa.edu.ng

DOI: https://doi.org/10.30564/jgr.v3i1.2805

reservoir quality. This problem is known as curse of dimensionality [3].

Regression analysis is the most commonly used technique to predict reservoir quality [4-6]. However, this technique has limitations and demands intense interaction with domain experts. Moreover, such models are sensitive to the limits imposed by the calibration dataset. Recently, soft computing techniques have been used in reservoir characterization and modeling [7]. Among these techniques, Artificial Neural Networks (ANNs) have been used to identify relationships between permeability, measured logs and core data [8].

In this paper, we propose the use of the stochastic modelling technique to predict reservoir quality indicators at and away from well locations. This enables more precise definition of reservoir geometry, prediction and evaluation of reservoir quality in and away from well locations and the eventual ranking of these realizations.

2. Location and Geology of the Study Area

The field is located within the Niger delta (Figure 1). The base map showed the location of the four wells and the seismic lines.

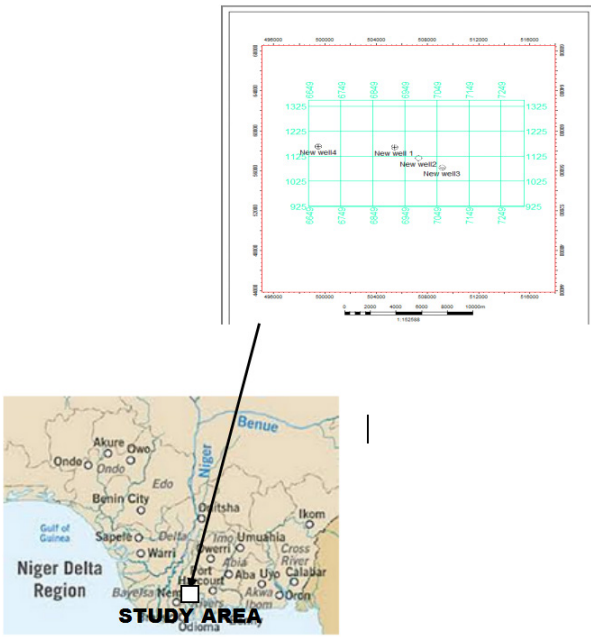

Figure 1. Map of Niger Delta showing the Study Area and Base Map

The Niger Delta basin is located on the continental margin of the Gulf of Guinea in equatorial West Africa and lies between latitudes 4° and 7°N and longitudes 3° E [9]. It ranks among the worlds' most prolific petroleum producing Tertiary deltas that together account for about 5% of the worlds' oil and gas reserves. It is one of the economically prominent sedimentary basins in West Africa and the largest in Africa [10]. Three lithostratigraphic units have been recognized in the subsurface of the Niger Delta [11-13]. These are, from the oldest to the youngest, the Akata, Agbada and Benin Formations. The Akata Formation (Eocene - Recent) is a marine sedimentary succession that is laid in front of the advancing delta and ranges from 1,968ft to 19,680ft (600-6,000m) in thickness. It consists of mainly uniform undercompacted shales with lenses of sandstone of abnormally high pressure at the top [13]. The shales are rich in both planktonic and benthonic foraminifera and were deposited in shallow to deep marine environment[11]. The Agbada Formation (Eocene-Recent) is characterized by paralic interbedded sandstone and shale with a thickness of over 3,049m [10]. The top of Agbada Formation is defined as the first occurrence of shale with marine fauna that coincides with the base of the continental-transitional lithofacies [14]. The base is a significant sandstone body that coincides with the top of the Akata Formation [11]. Some shales of the Agbada Formation were thought to be the source rocks, however; [15] deduced that the main source rocks of the Niger Delta are the shales of the Akata Formation.

The Benin Formation is the youngest lithostratigraphic unit in the Niger Delta. It is Miocene - Recent in age with a minimum thickness of more than 6,000 ft (1,829m) and made up of continental sands and sandstones (>90%) with few shale intercalations. The sands and sandstones are coarse grained, subangular to well rounded and are very poorly sorted.

3. Methodology

The flow chart used for the data analysis is as shown below in Figure 2.

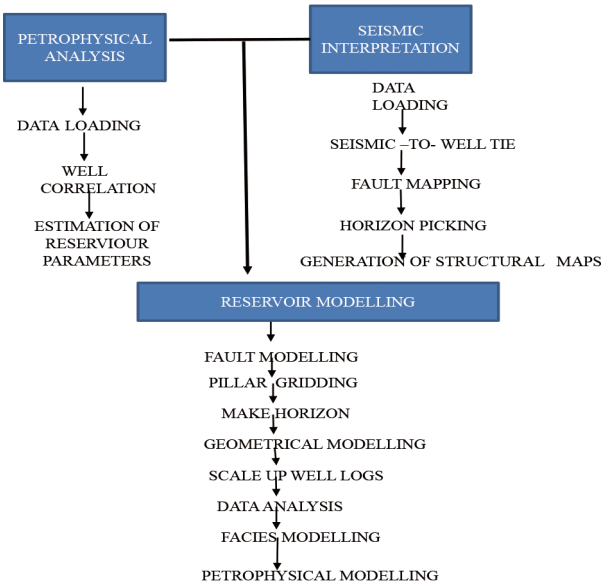

Figure 2. Flow Chart used for Data Analysis

 DOI: https://doi.org/10.30564/jgr.v3i1.2805

Geostatistical Modelling

3.1 Variogram Analysis

A variogram was used as input when discrete property was populated using a stochastic algorithm. The mathematical definition of the variogram is:

$$(h) = \frac{1}{2m}\sum_{i=1}^{m}[(x_i) - Z(x_i + h)]^2 \quad (1)$$

where m is the number of pairs of sample points of observations of the values of attribute Z separated by distance (lag) h.

A normal score (Gaussian) transformation was applied to the upscaled logs to normalise the data prior to variogram analysis. This was done so that the variables will achieve stationarity. This means that statistical properties do not depend on exact positions [18]. Spherical and Gaussian models were applied to the variograms. The variogram analyses were carried out for all the zones in three directions. The major direction is Northwest-Southeast (NW-SE) being the trend of the rollover structure in the study area. The minor direction (Northeast-Southwest, NE-SW) is perpendicular to the major direction while the vertical direction conforms to depth.

Generally the Steps Involved in Populating Data Away from Well Bore Involves:

(1) Carrying out variogram analysis for the 4 wells which involves: calculating experimental variogram (average of the squared difference between nodes (point pairs) to obtain a single value of variance for that specific "lag distance". The plot of the variance and the lag distance produced the experimental variogram

(2) Fitting a curve (Spherical, Exponential, Gaussian) along the experimental variogram to get Model Variogram to obtain the (Nugget, Sill, Range)

(3) Krigging of the available property values to obtain a value for the unknown point

(4) Plotting of cumulative frequency curve (Ogive) where different percentile values will give rise to different realizations (iterations) for the same surface.

3.2 Ranking of Realizations

The five realizations of the properties modelled were ranked in other to choose the realization that is close to the control values using a statistical tool called Lp norm using the second order which is the least square method.

This method averages the deviation from the true value and estimate the error. The realization with the least error is taking as the best which can be used for further analysis. The expression is as stated below.

$$L_p norm = \sum_{n=1}^{\infty}\frac{(d_{true} - d_{realization})^2}{n} \quad (2)$$

4. Results and Discussion

Figure 3 depicts variation in thickness of Sand X across the four wells. Table 1 reveals that it is thickest in Well 4 (73.2 m) and thinnest in Well 1 (13,3 m). Also, the sand body is cleanest in Well 4 (Vsh = 0.09) and dirtiest in well (Vsh = 0.4). These are further supported by the observed relative sand-shaleproportion in these wells. The deep resistivity log readings are high across the wells, indicating that they are all hydrocarbon-bearing. The thick column of shale overlying and underlying the sand, serves as good seal.

The net thickness, which is the amount of sand within Sand 2 ranges from 11.77m to 60.64m while, the net pay thickness has a range of 5.44m to 43.36m and these initial values gave high net to gross range for Sand 2 to be from 0.78 to 0.89.

The porosity and permeability values ranged from 0.20 to 0.32 and 1000mD and 3122mD respectively. Due to the high net- to- gross values, we have corresponding low volume of shale values ranging from 0.09 to 0.40. Sand X is hydrocarbon bearing in all the wells because of the low water saturation and high hydrocarbon saturation values.

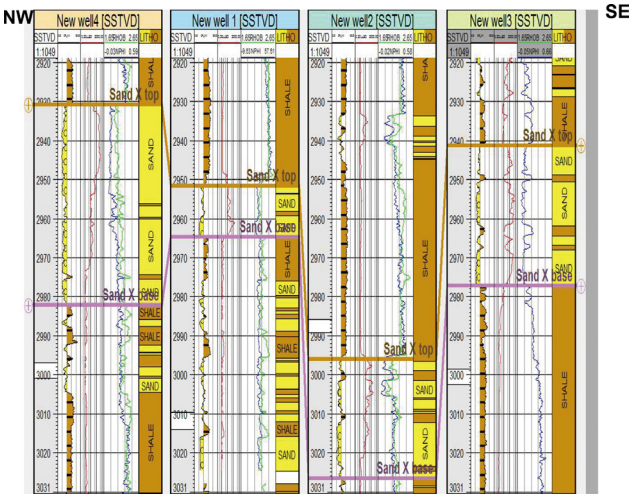

Figure 3. Well Correlation Panel showing the Top and Base of Sand X

Table 1. Petrophysical Parameters for Sand X

SAND 2	Gross (m)	Net (m)	Net Pay (m)	N/G	Ø	K (mD)	V_{sh}	S_w	S_h
WELL 1	13.27	11.77	5.44	0.89	0.23	1452	0.09	0.31	0.69
WELL 2	30.63	23.90	20.59	0.78	0.32	3122	0.15	0.38	0.62
WELL 3	35.81	30.79	30.79	0.86	0.20	1000	0.21	0.43	0.57
WELL 4	73.19	60.64	43.36	0.86	0.25	2883	0.40	0.20	0.80

DOI: https://doi.org/10.30564/jgr.v3i1.2805

4.1 Seismic Interpretation

Seimic data was interpreted in order to unravel the underlying geology that gave rise to observable reflections. Seismic-to-well tie ,Figure 4, was carried out to ensure correct horizon mapping. The time structural map of the top of Sand X, Figure 5, with a TWT range of around 2820ms to 3320ms and a contour interval of 30ms. There is a structural high from the central to the nothern part of the field, and another small closure on it; justifying the probable location of the wells.

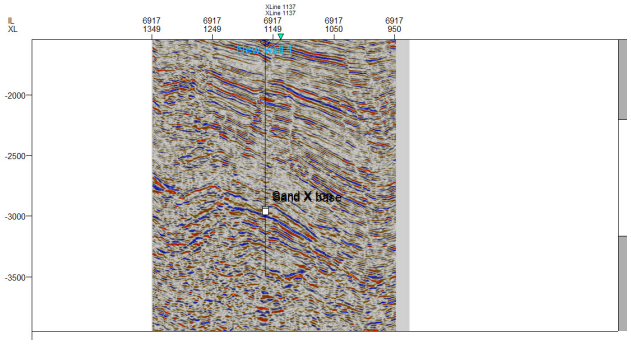

Figure 4. Seismic-to-Well tie shown on inline 6917

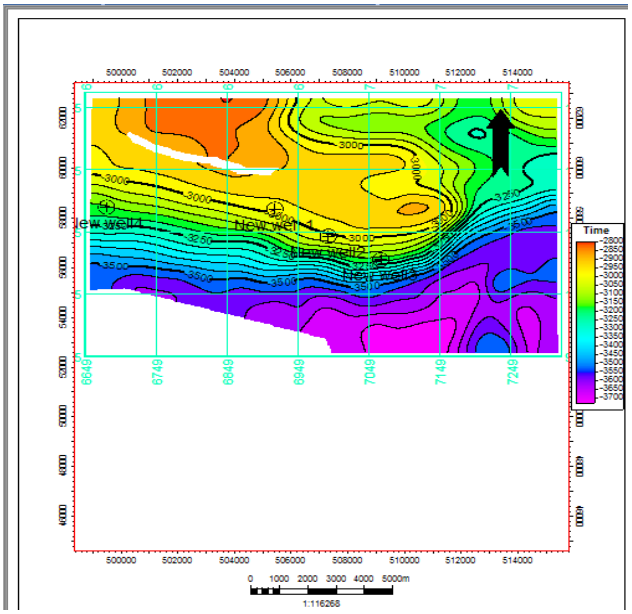

Figure 5. Time Structural Map of Top of Sand X

4.2 Reservoir Modelling

4.2.1 Volume of Shale Model for Sand X

Thus far, reservoir quality information has been very sparse; available only at well locations. The Geostatistical reservoir modelling exercise facilitated wider distribution of the computed reservoir quality indicators away from these well locations. Prior to the modelling, variogram analysis was done and the nugget and sill values were close to 0 and 1 respectively. The first realization of volume of shale model in Sand X (Figure 6) shows the variation of the property across the field. The low volume of shale at and around the well locations lend further credence to the presence hydrocarbon as well as high reservoir quality. The volume of shale values at the location of Wells 4 and 1 are lower than those of the remaining two wells. High volumes of shale values are present at the central, southwestern and southeastern parts of the field.

The second realization in Figure 7 shows a distribution different from the first realization with low volume of shale values at the western, central to the northern parts. A higher volume of shale could be observed around the south-eastern flank of the field. This connotes higher presence of shale anda resultant reduction in reservoir quality. Figure 8 shows the third realization with low volume of shale values at the existing well locations and high volume of shale values scattered around them.

In the fourth realization shown in Figure 9, there is a lit bit high volume of shale value around Well 4 and other well locations, however there are clusters of low volume of shale values around them. In the fifth realization (Figure 10), there are high volume of shale at the edge of the western part and clusters of low volume of shale values at the northeastern and toward the western portion.

Based on the statistical ranking, equation 2, and Table 2, the first realization is adjudged best of the five. It contains the least error and therefore of best reservoir quality.

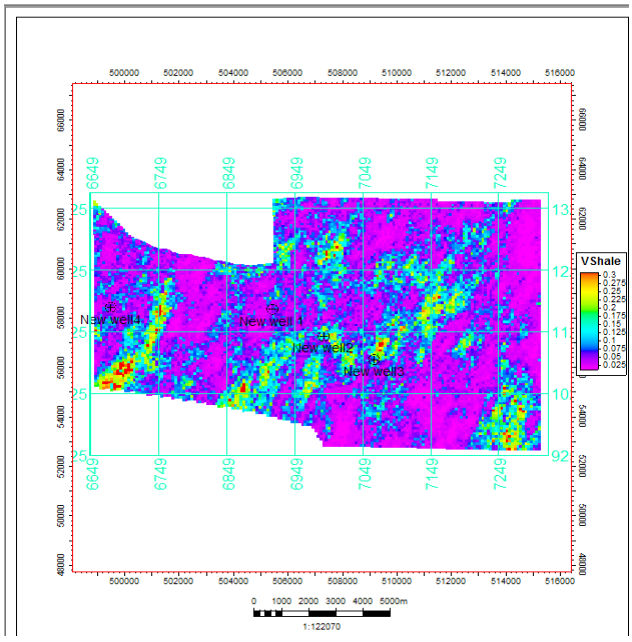

Figure 6. Model of Volume of Shale Distribution in Sand X (1st Realization)

DOI: https://doi.org/10.30564/jgr.v3i1.2805

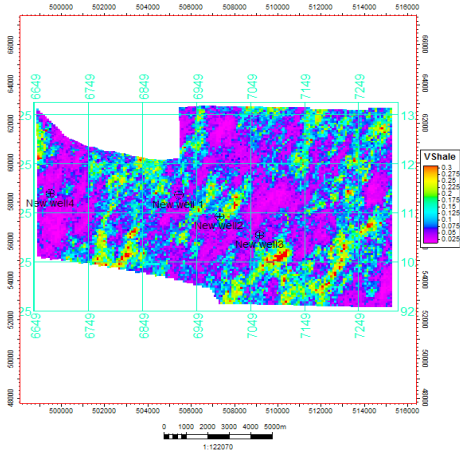

Figure 7. Model of V. Shale distribution in Sand X (2nd Realization)

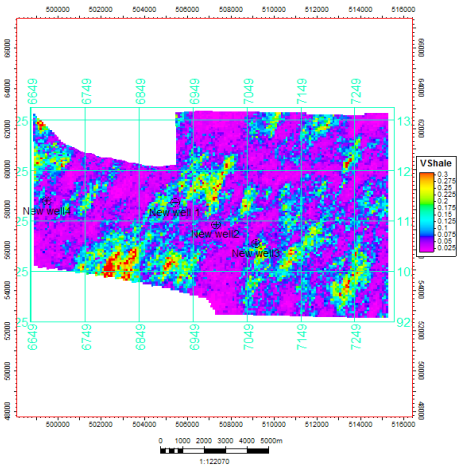

Figure 8. Model of V. Shale distribution in Sand X (3rd Realization)

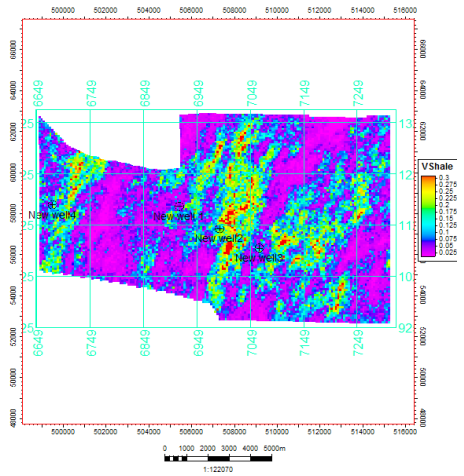

Figure 9. Model of V. Shale distribution in Sand X (4th Realization)

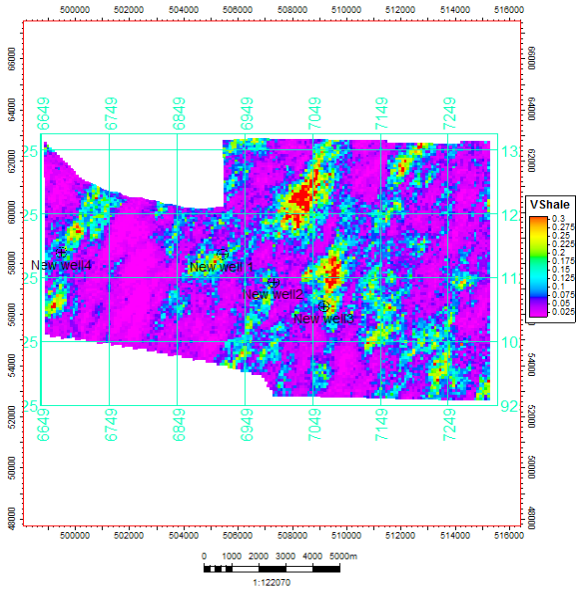

Figure 10. Model of V. Shale distribution in Sand X (5th Realization)

Table 2. Volume of Shale Values at Well Locations for the 5 Realizations and the Control

VSHF2	WELL 1	WELL2	WELL3	WELL4
1st Realization	**0.05**	**0.18**	**0.1**	**0.03**
2nd Realization	0.025	0.075	0.15	0.035
3rdRealization	0.07	0.045	0.12	0.056
4thRealization	0.041	0.12	0.175	0.053
5thRealization	0.05	0.08	0.095	0.057
CONTROL	**0.09**	**0.15**	**0.21**	**0.40**

Similarly, Figures 11 and 12 showed the best of the five realizations for the net-to-gross, effective porosity respectively. The permeability model, Figure 14 was distributed using a crossplot of permeability against porosity Figure 13.

4.2.2 Net to Gross Model for Sand X

The best realization for net-to-gross model was observed at fourth realization. At all the well locations, Figure 10, very high values of net-to-gross were observed.

The model showed the highest net -to -gross value in Well 1 (0.92) and lowest in Well 3 (0.82) with clusters of high net -to- gross values exist toward the western and eastern part of the field, and low net to gross values exist around Wells 1 and 2. These high values depict low level of shale in the reservoir; which favours high reservoir quality.

Table 3 contains the numerical values extracted from

DOI: https://doi.org/10.30564/jgr.v3i1.2805

the well locations for the five realizations and the values are favourably okay for a good reservoir with the fourth realization values close to that of the control.

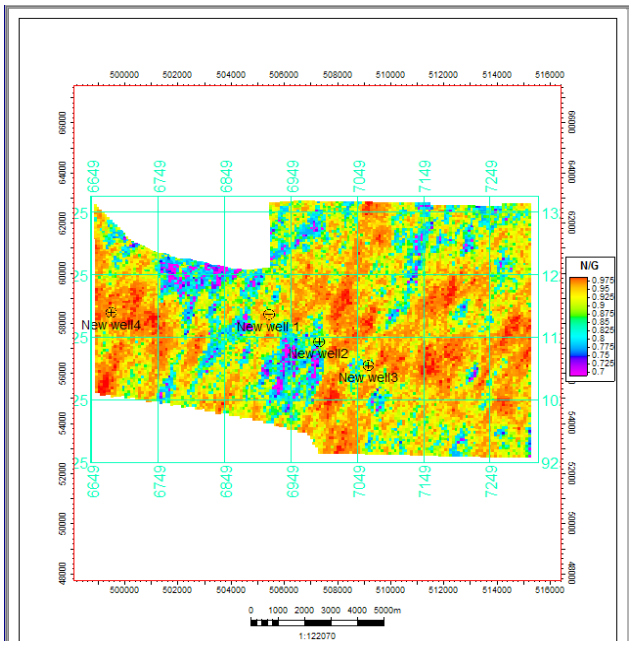

Figure 11. Model of N/G distribution in Sand X (4th Realization)

Table 3. Net to Gross Values at Well Locations for the 5 Realizations and the Control

NTG2	WELL 1	WELL2	WELL3	WELL4
1st Realization	0.92	0.83	0.85	0.95
2nd Realization	0.94	0.87	0.83	0.94
3rdRealization	0.93	0.89	0.81	0.96
4thRealization	**0.92**	**0.86**	**0.82**	**0.89**
5thRealization	0.86	0.84	0.91	0.93
CONTROL	**0.89**	**0.78**	**0.86**	**0.86**

4.2.3 Effective Porosity Model for Sand X

The best realization of effective porosity model is shown in Figure 12. The effective porosity values varied from Well 4 (29%) to 15% in Well 3. There are packets of low effective porosity values at the northern part and around Wells 1 which spreads to Well 3 location. The Western and South-eastern flanks of the reservoir exhibit high effective porosity , which supports the net-to-gross revelations. Again, the reservoir quality is adjudged reasonably acceptable across the reservoir. The numerical values extracted from the well locations for the five realizations are shown in Table 4 and the first realization with a range of 0.14 to 0.29 is close to the control values. High effective porosity values are expected for a good hydrocarbon bearing reservoir.

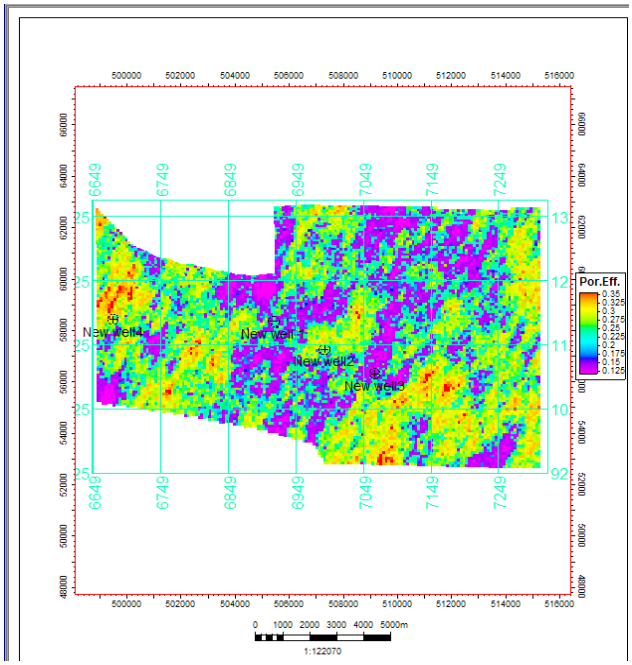

Figure 12. Model of PHIE Distribution in Sand X (1st Realization)

Table 4. Effective Porosity Values at Well Locations for the 5 Realizations and the Control

Eff. Por.2	WELL 1	WELL2	WELL3	WELL4
1st Realization	**0.25**	**0.27**	**0.14**	**0.29**
2nd Realization	0.23	0.26	0.15	0.32
3rdRealization	0.275	0.27	0.12	0.33
4thRealization	0.26	0.22	0.13	0.28
5thRealization	0.25	0.26	0.125	0.295
CONTROL	**0.23**	**0.32**	**0.20**	**0.25**

4.2.4 Permeability Model for Sand X

There exist strong relationship between permeability and porosity[17,18] . Consequently a crossplot of permeability and porosity, Figure 13, was generated values to deduce this relationship for Sand X. The relationship is as shown in equation 3

$$K = 57821.9 * Ø - 9990.7 \quad (3)$$

Where K is the permeability and **Ø** is the porosity, an increase in porosity produces a corresponding increase in permeability.

This equation was then used with the initial porosity model, Figure 12, to generate the permeability model in Figure 14. It shows the variation in permeability across the field. Expectedly, high permeability values were ob-

DOI: https://doi.org/10.30564/jgr.v3i1.2805

served in and around Wells 4, 1 and 2, while a relatively low was observed around Well 3. This reasonably reflects the findings of the effective porosity model affirming high quality of the reservoirThere are clusters of high permeability values at the western, central and southern parts of the model.

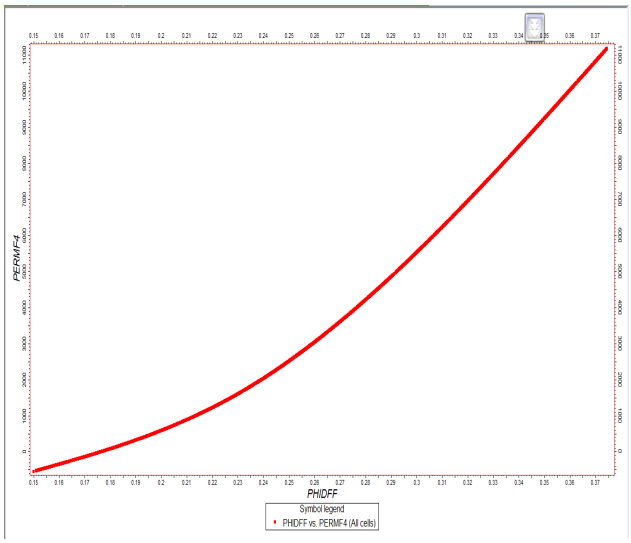

Figure 13. Crossplot of Permeability and Total Porosity

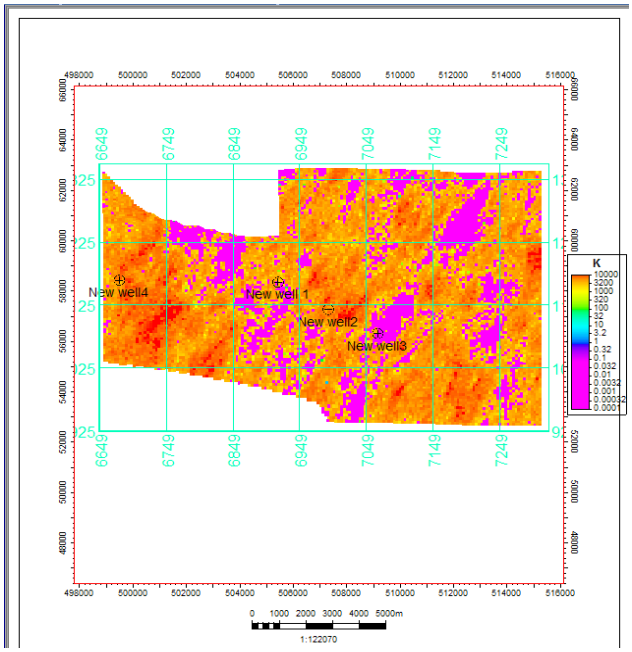

Figure 14. Model of Permeability distribution in Sand X

5. Conclusion

The study has employed surface seismic and well data to determine the reservoir quality at the well locations and geostatistically away from them.The reservoir quality indicators that were modelled stochastically showed variation in the distribution of volume of shale, effective porosity, net to gross and permeability within the field. At the existing well locations the reservoir quality were good based on the values. Away from well bore, for some realizations, the reservoir quality improves while it decreased in others. Regions beyond the existing well locations with good property values are good targets for hydrocarbon exploitation. The one realization for the permeability model also displayed variation in permeability across the field. Areas with high effective porosity, low volume of shale, high net to gross and high permeability are deemed to be of good quality which could further be explored.

References

[1] Kupecz, J.; Gluyas J., Block, S. Reservoir quality prediction in sandstones and carbonates: An Overview. In: Kupecz J., GluyasJ. and Block S. (Eds). Reservoir quality prediction in sandstones and carbonates, AAPG Memoir 69, 1997.

[2] Fanchi, J. R. Principles of Applied Reservoir Simulation. 2nd ed., MA, USA, Elsevier Burlington, 2001.

[3] Bellman, R., Dreyfuss, S. Applied Dynamic Programming. Princeton, USA, Princeton University Press, 1962.

[4] International energy agency. World energy outlook, 2007

[5] Love, K. M., Strohmenger, C., Woronow, A., Rockenbauch, K. Predicting Reservoir Quality Using Linear Regression Models and Neural Networks. 1997.

[6] Bloch, S. Empirical predictions of porosity and permeability in sandstones. AAPG Bulletin, 1991, 75: 1145-1160.

[7] Nikravesh, M., Aminzadeh, F., Zadeh, L. A. Soft computing and intelligent data analysis in oil exploration. Ney York, USA, Elsevier, 2003.

[8] Ligtenbert, J. H., Wansink, A. G. Neural Network Prediction of permeability in the El Garia Formation, Ashtart Oilfield, Offshore Tunisia. In: Nikravesh M., Aminzadeh F., Zadeh, L.A (Eds). Developments in Petroleum Science, 2003, 51: 397-411.

[9] Whiteman, A. Nigeria: Its petroleum geology, resources and potential: London. Graham and Trotman,1982; 381 .

[10] Reijers TJF. Selected Chapters on Geology, SPDC of Nigeria, Corporate Reprographic Services, Warri., 1996, 197.

[11] Short KC, Stauble, J. Outline geology of the Niger Delta. AAPG. 1967, Bull 5: 761-779

[12] Frankl, E.J., Cordy, E.A. The Niger Delta Oil Province Recent Development Onshore and Offshore, 7thWorld Petroleum Congress Proceedings, Mexico

DOI: https://doi.org/10.30564/jgr.v3i1.2805

City, IB, 1967: 195-209.
[13] Avbovbo, A. A., Tertiary lithostratigraphy of Niger Delta: American Association of Petroleum Geologists Bulletin, 1978, 62: 295-300.
[14] Adesida A, Ehirim, BO. Cenozoic Niger Delta: A guide to its lithosedimentary analysis. SPDC Exploration note 88.002 (Ref: on-shore wells), 1988, 1-10.
[15] Ejedawe, J.E., S.J.L.Coker, D.O. Lambert-Aikhionbare, K.B. Alofe, F.O. Adoh. Evolution of Oil Generating Window and Gas Occurrence in Tertiary Niger Delta Basin. AAPG Bull, 1984, 68: 1744-1751.
[16] Deutsch, C.V. Geostatistical Reservoir Modeling. Oxford University Press, 2002: 376.
[17] Etu-Efeotor, J.O. Fundamentals of petroleum geology. Paragraphic publications, Port Harcourt, Nigeria, 1997, 135.
[18] Adeoti, L., Njoku, O., Olawale, O., Fatoba, J., Musa, B. Static Reservoir Modelling using Well Log and 3-D Seismic Data in a KN Field, Offshore Niger Delta, Nigeria. International Journal of Geoscience, 2014, 5: 99-106.

 DOI: https://doi.org/10.30564/jgr.v3i1.2805